Utilizing of Static Synchronous Compensator for Reducing the Output Harmonic Distortions of Wind Turbines

Sima Jafarzadeh [1], Saeed Barghandan [2], Mohsen Ebadpour [3]
Department of Electrical Engineering. Ahar Branch, Islamic Azad University, Ahar, Iran
Email: saeed_barghandan@yahoo.com [2] (Corresponding author)
Email: sima.jafarzadeh@yahoo.com [1], m-ebadpour@iau-ahar.ac.ir [3]

Abstract

Due to the variable and non-uniform nature of wind speed, using the variable speed wind power plants equipped with induction generators has advantages over the fixed speed wind power plants; however, it also contains some disadvantages such as consuming a large amount of reactive current in the power grid and causes voltage drop and instability. The use of static synchronous compensator or STATCOM is one of the key methods to improve the power profile in wind farms. STATCOM can control the voltage dynamics, improve transient stability, eliminate power fluctuations in the transmission network, and control the real and reactive power. Regarding to the fluctuations in electricity generated in wind farms, the presented case study proposed methods to improve the active power and compensate reactive power using the STATCOM in wind systems by modeling in Simulink environment of MATLAB software. According to the simulation results, by applying the STATCOM to the studied system, changes in active power and reactive power generated from the wind farm are significantly reduced. In addition, studies in terms of total harmonic distortion (THD) show that by employing STATCOM, the amount of output voltage distortion is vastly decreased.

Keywords: Wind turbine, static compensator, STATCOM, reactive power, harmonic distortion.

1. Introduction

The tendency of countries around the world to use renewable energy such as wind energy, as the main source of electricity production, in recent years has been considered. A wind power plant or wind farm is a collection of several wind turbines located in one place. Significant progress has been made in the development of wind turbines to generate electricity since 1975, and around 1980 the first modern turbines were connected to the power grid [1]. With the expansion of the use of wind energy and wind power generation, wind turbines connected to double fed induction generators are widely used [2]. At the end of 2010, the nominal capacity of wind power generation in worldwide was 197 GW. Today, wind power in the world has an annual production capacity of 430 TW of electricity, which is 2.5% of world electricity consumption [3].

Using the variable speed wind turbines has advantages over fixed speed wind power plants. Although fixed speed wind farms can be connected directly to the grid, a wider range of energy is covered by variable speed wind farms. Lack of reactive power in power grids causes voltage drop and voltage fluctuations. Due to the expansion and complexity of power grids, reactive power compensation is a key in order to prevent voltage collapse. The use of static compensator or STATCOM is one of the methods used to improve power in wind farms. Inverter has been used in this compensator to provide the required reactive power locally and its output is continuously adjustable. Using STATCOM, it is possible to have dynamic voltage control, improve transient stability, eliminate power fluctuations in the transmission network, and control real and reactive power [4].

In the past, to compensate the reactive power of the power grid, wind turbines were connected directly to the power grid and the required reactive power was supplied through the grid [5]. In [6], a 24 pulses three-level static synchronous compensator with pulse width modulation (PWM) control method is presented to work in main frequency. In this method, four three-level Voltage Source Converters (VSC) and four identical transformers are used to control the reactive power using a current control algorithm that has a complex circuit. In [7], the voltage sensitivity of the grid over the reactive power conditions is analyzed and STATCOM is used to improve the voltage profile of different buses. Due to the rapid dynamic response of this method, in addition to improving voltage levels, the damping rate of voltage fluctuations has also increased. In [8], besides examining the issues such as control of voltage, frequency, reactive power, dynamic load fluctuations as well as power quality issues for the dynamic stability of the synchronous generator connected to the network are discussed using FACTS devices.

In [9], the coordination of a coil equipped with superconducting energy storage system (SMES) with a STATCOM compensator is studied in order to improve the transient stability and damping of dynamic fluctuations in the power system. In this system, the performance principles of the hybrid compensator, its effective performance in the field of transient stability correction and attenuation of power fluctuations through modeling on a system with STATCOM compensator have been evaluated. In [10], a STATCOM with passive filter is used to improve the power quality of Tehran metro network. In [11], STATCOM transient performance improvement with energy storage systems is discussed. By combining STATCOM and battery energy storage, system performance can be significantly improved. In [12], the conventional solutions to increase the capacity of transmission lines due to the existing limitations are discussed. Finally, by simulating a 14-bus system and applying a short-circuit fault in it, the importance of compensation to achieve a flat voltage profile curve with the presence of STATCOM is analyzed.

In this paper, power improvement and reactive power compensation using STATCOM in wind farms are investigated. The proposed system is able to control the active power in a wide range and the reactive power output changes in the wind farm with STATCOM with an acceptable level. Moreover, by using STATCOM, the amount of harmonic distortion of current and output voltage is greatly reduced. In the second part, the modeling of double fed induction generator as wind energy generator is discussed. The structure and function of STATCOM are described in Section 3. In the fourth part, the control strategy of the studied system is presented along with their equations. Finally, the simulation results of the system under different operating conditions are shown.

2. Modeling of Wind Generator

In order to explain the characteristics and methods of controlling of wind turbines, it is necessary to model their generators. For this purpose, in this section, first, the modeling of the wound induction machine is discussed. Figure 1 shows the schematic of the rotor and stator windings of an induction machine with a wound rotor [13].

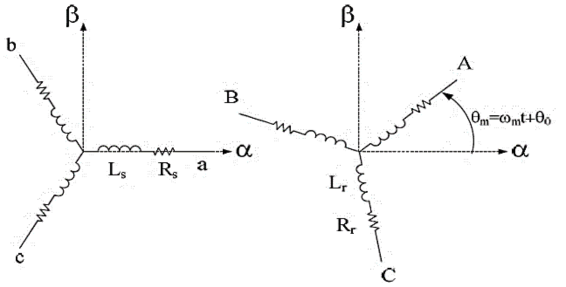

Fig. 1. Schematic of rotor and stator windings of induction machine with wound rotor.

The current and voltage equations for each of the rotor and stator windings are expressed as follows

$$\begin{cases} v_s = R_s i_s + \dfrac{d\psi_s}{dt} \\ v_r = R_r i_r + \dfrac{d\psi_r}{dt} \end{cases} \tag{1}$$

Assuming the zero sequence component is zero, all variables can be written using Equation (2) as the following space vector

$$f_{\alpha\beta} = f_\alpha + jf_\beta = \frac{2}{3}\left(f_a + e^{j\frac{2\pi}{3}} + e^{-j\frac{2\pi}{3}} f_c \right) \tag{2}$$

$$\begin{cases} \vec{v}^{\,s}_{s,\alpha\beta} = R_s \vec{i}^{\,s}_{s,\alpha\beta} + \dfrac{d\vec{\psi}^{\,s}_{s,\alpha\beta}}{dt} \\ \vec{v}^{\,r}_{r,\alpha\beta} = R_r \vec{i}^{\,r}_{r,\alpha\beta} + \dfrac{d\vec{\psi}^{\,r}_{r,\alpha\beta}}{dt} \end{cases} \tag{3}$$

It can be written regardless of magnetic losses

$$\begin{bmatrix} \vec{\psi}^{\,s}_s \\ \vec{\psi}^{\,r}_r \end{bmatrix} = \begin{bmatrix} L_s & L_m \\ L_m & L_r \end{bmatrix} \begin{bmatrix} \vec{i}^{\,s}_s \\ \vec{i}^{\,r}_r \end{bmatrix} \tag{4}$$

If the current and voltage equations of the rotor and stator are transferred to the rotating reference frame with speed ω_k, they can be rewritten as folows

$$\begin{cases} \vec{v}^{\,k}_s = R_s \vec{i}^{\,k}_s + j\omega_k \vec{\psi}^{\,k}_s + \dfrac{d\vec{\psi}^{\,k}_s}{dt} \\ \vec{v}^{\,k}_r = R_r \vec{i}^{\,k}_r + j(\omega_k - \omega_m)\vec{\psi}^{\,k}_r + \dfrac{d\vec{\psi}^{\,k}_r}{dt} \end{cases} \tag{5}$$

The output power equations of stator and rotor can be calculated from the following equations.

$$P_s = \frac{3}{2}\mathrm{Re}\left\{ \vec{v}^{\,k}_s \vec{i}^{\,k*}_s \right\} \tag{6}$$

$$P_r = \frac{3}{2}\mathrm{Re}\left\{ \vec{v}^{\,k}_r \vec{i}^{\,k*}_r \right\} \tag{7}$$

The electricomagnetic torque of the machine can be calculated according to (8)

$$T_e = -\frac{3}{2} n_P \,\mathrm{Im}\left\{ \vec{i}_r \vec{i}^{\,*}_s \right\} = -\frac{3}{2} n_P L_m \vec{i}_s \times \vec{i}_r \tag{8}$$

where n_P is the number of machine pole pairs.

The above equations, in addition to the mechanical equation of the induction machine as (9), describe the complete model of the induction generator.

$$T_m - T_e = j\frac{d\omega_m}{dt} + B\omega_m \tag{9}$$

3. Static Synchronous Compensator

The basis of STATCOM operation is similar to a synchronous condenser. Since power electronic devices are used in STATCOM structure, it is called a static compensator. The converters used in this compensator provide the required reactive power locally and its output is continuously adjustable, therefore, in cases where the main voltage has wide variations, this compensator is used. The various parts of a STATCOM, shown schematically in Fig. 2, include a transformer, converter, DC capacitor, energy storage, and controller. The AC side current is a fully reactive and does not exchange any active power with the grid, so the ideal DC side current is zero. But in fact, this current is a small amount that changes in proportion to the converter ripple. Therefore, the capacitance of the DC side capacitor must be selected in proportion to the converter ripple.

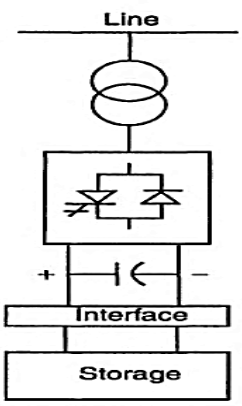

Fig. 2. Different parts of a STATCOM.

The system controller commands the converter according to the measured values, reference inputs and parameter setting, and controls the amplitude of the injected reactive power. The required reactive power is supplied through a capacitor. STATCOM receives DC voltage through a capacitor and converts it to AC voltage with a converter capable of controlling amplitude and phase angle. The STATCOM single line structure is shown in Fig. 3. STATCOM performs two-way voltage conversion, which can be used temporarily to absorb or generate active power.

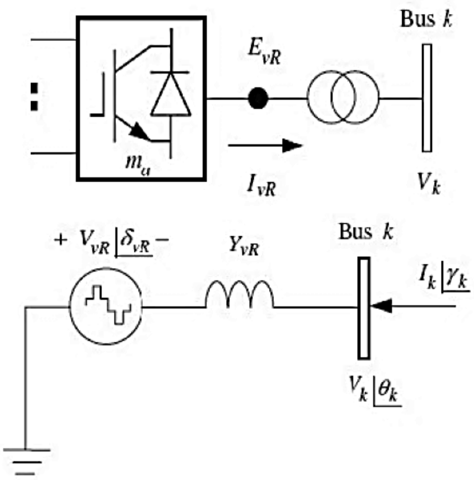

Fig. 3. Single-line model of STATCOM.

4. Control Strategy

The basic structure of a STWCOM with PWM-based voltage control is shown in Fig. 4. The STATCOM model which presented here is based on the power balance equation, that basically represents the balance between the AC power expressed in Equation (11) and the DC power under equilibrium conditions at the main frequency.

$$P = P_{dc} + P_{loss} \tag{10}$$

PMW control is a practical factor for VSC-based controllers because with recent advances and the advent of the GTO, they no longer have high switching losses. Assuming the voltages are balanced, the system transient control method for transient stability studies is shown in Fig. 5.

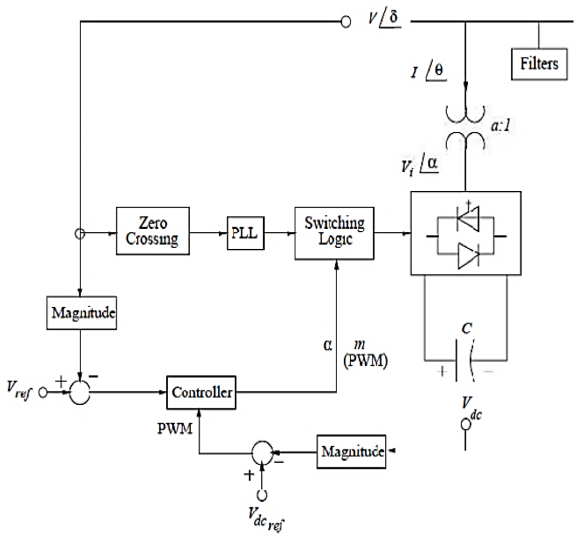

Fig. 4. Block diagram with PWM voltage control.

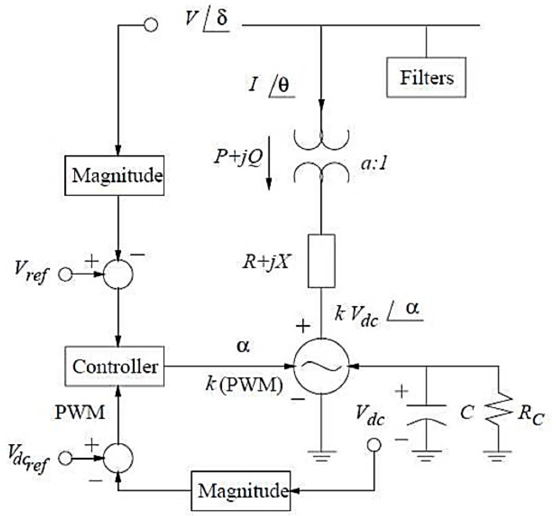

Fig. 5. STATCOM transient stability model with PWM voltage control.

The differential equations for the transient model can be written as follows

$$\begin{bmatrix}\dot{x}_c\\ \dot{\alpha}\\ \dot{m}\end{bmatrix} = f_c(x_c,\alpha,m,V,V_{dc},V_{ref},V_{dc_{ref}}) \quad (11)$$

$$\dot{V}_{dc} = \frac{VI}{CV_{dc}}\mathrm{Cos}(\delta-\theta) - \frac{G_C}{C}V_{dc} - \frac{R\ I^2}{c\ V_{dc}} \quad (12)$$

The admittance $(R+JX)^{-1} = G + JB$ represents the impedance of the transformer and each AC series filter. G_c is used for modelling the inertia of the converter cused by its electronic switches and circuits, which has a direct effect on the voltage dynamics of the capacitor. The variables x_c in Equation (11) is the variable of the internal control system, therefore highly dependent on the PWM or phase control method used in the presented controller.

In the simple voltage controller shown in Fig. 6, the variables and differential equations are directly related to the various control blocks. It can be seen that in this PWM controller, the AC bus voltage range is controlled by the modulation index *m* and this has a direct effect on the VSC voltage range. The phase angle α basically determines the active current flow in the controller and is also used for charging and discharging the capacitor to directly control the DC voltage range.

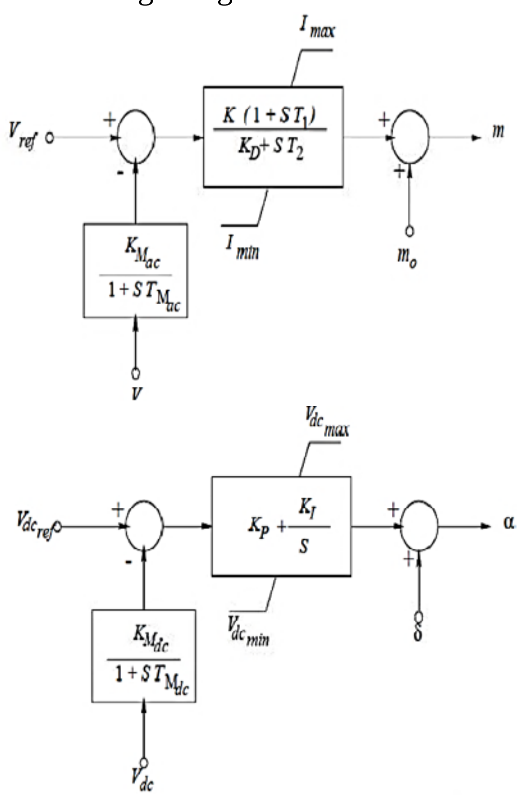

Fig. 6. PWM voltage control of a STATCOM.

It should be noted that the controllers have a bias that is related to the value of the constant state of the modulation index m_0 for the voltage amplitude controller and also to the STATCOM output phase angle for the DC voltage controller. The steady state model can be easily obtained from the previous equation by placing the differential equations corresponding to the DC voltage steady state equations and the STATCOM voltage control charactristics.

The general scheme of generating power from wind based on the use of asynchronous generators simulated in MATLAB software is presented in Fig. 7. In equations and models of wind turbines, the amount of wind power is determined by the following equation

$$P_m = C_p P_w \qquad (13)$$
$$P_w = \frac{1}{2}\pi\rho R^2 v_w^3$$

where P_m represents the mechanical power of wind turbine, P_w wind power, ρ air density, R radius of turbine blades, v_w wind speed in meters per second and C_p efficiency coefficient. The efficiency coefficient C_p determines the percentage or part of the energy in the wind that can be extracted by the turbine [14].

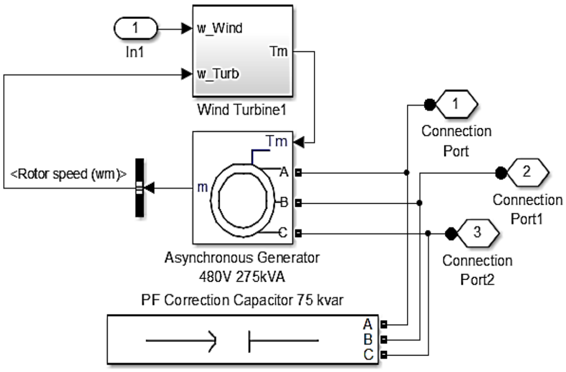

Fig. 7. Wind turbine model with asynchronous generator.

If the optimal relationship between turbine speed and wind speed is maintained by changing the wind speed, the maximum power output from the wind will be guaranteed. For wind speeds $4\,m/s$ and $12\,m/s$ generator speeds to get the maximum power is approximately $(1\pm 50\%)\omega_{sync}$, which is actually the range of speed changes. The blade angle controller is activated for higher speeds than $12\,m/s$, otherwise the generators and converters will be overloaded. In simulating a wind turbine, the torque produced at different speeds is required to be applied to the generator. Turbine output torque can be calculated with the following equation

$$T_a = \frac{P_m}{\omega_t} = \frac{1}{2}\frac{\rho\pi R^2 C_p v^3}{\omega_t} \qquad (14)$$

5. Simulation Results

In this section, the results of wind farm modeling which includes four wind turbines in the presence of STATCOM are presented. These results include current, voltage, active power and reactive power. Since the simulation time interval is 10 seconds, the output waveforms are illustrated in magnification mode and in different time intervals.

The output voltage of the system rectifier is shown in Fig. 8. According to this figure, at the beginning of modeling and up to 2 seconds, the output voltage of the rectifier is increasing and then for a period of time has a decreasing trend of 2.5 and then the output voltage of the rectifier remains almost constant.

Fig. 10 shows the output voltage of STATCOM. It can be clearly seen that the output voltage from STATCOM has acceptable stability.

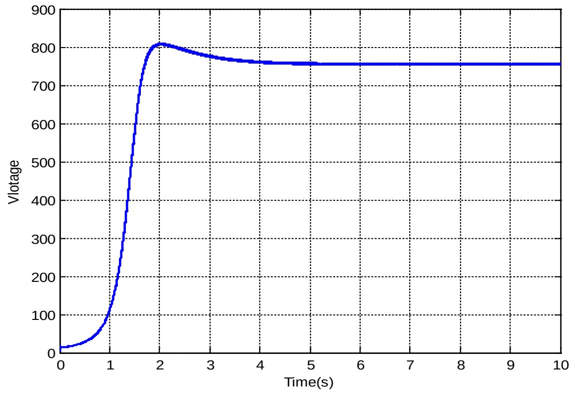

Fig. 8. Rectifier output voltage.

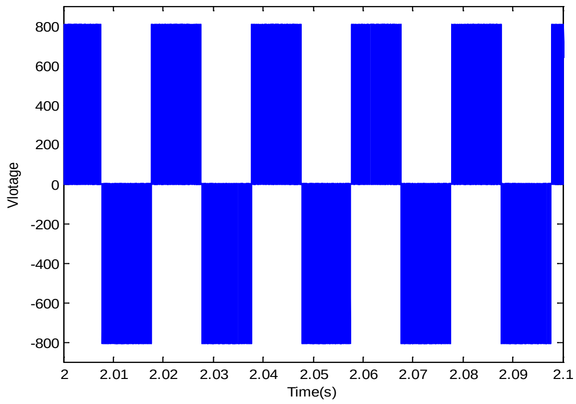

Fig. 9. Output voltage from STATCOM during 2 to 2.1 seconds.

With the increase of harmonics in the power grid, various standards were introduced to improve the quality of the power. These standards impose restrictions on harmonic injection by nonlinear loads into the grid. The most basic and common method for this purpose is to use passive LC filters. With the development of technology for making power semiconductor components, active filters were considered and used. In these filters, the effect of nonlinear loads is reduced by proper injection of current voltage. Figure 10 shows the output voltage of the LC filter. According to the output voltage of the LC filter, the high efficiency of the filter in harmonic reduction can be clearly seen.

Fig. 11 shows the output current of the LC filter. According to the figure, the output voltage and current of the LC filter are in a good match and coordination.

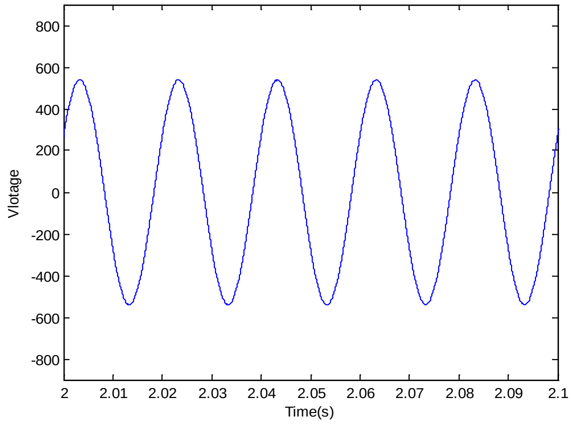

Fig. 10. Output voltage from LC filter during 2 to 2.1 seconds.

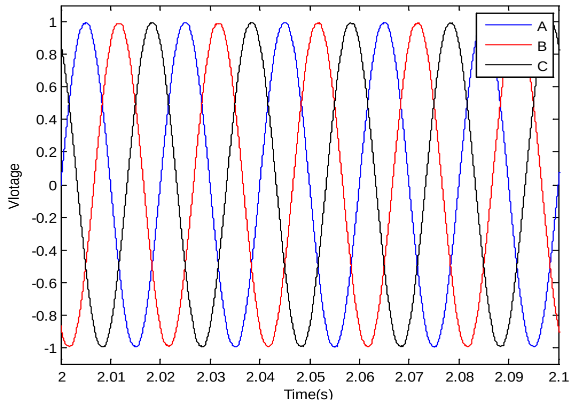

Fig. 11. Output current from LC filter during 2 to 2.1 seconds.

Fig. 12 shows the active and reactive power of the wind farm output with the presence of STATCOM.

For further investigation, the THD value of the output current and voltage from the wind farm are evaluated in the presence of STATCOM and the results are presented in Figs 13 and 14. In the output current, the value of THD is equal to 23.88% and in the output voltage, its value is equal to 23.9%, which is much reduced compared to the current and output voltage of the wind farm without STATCOM.

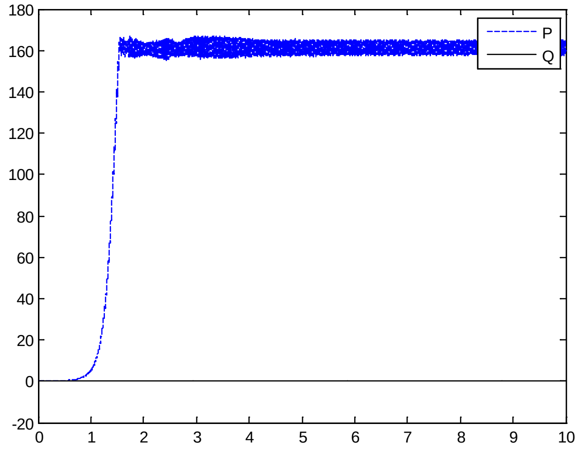

Fig. 12. Active and reactive power output of wind farm with the presence of STATCOM.

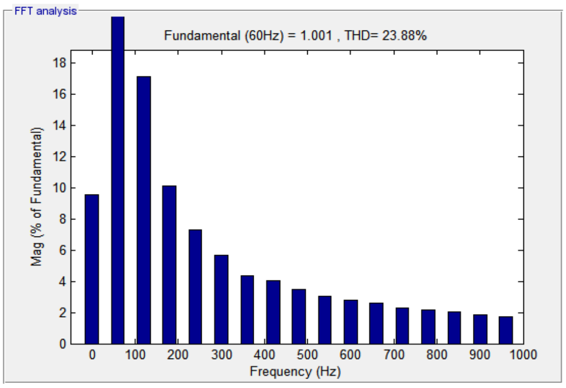

Fig. 13. THD of output current from the wind farm in the presence of STATCOM.

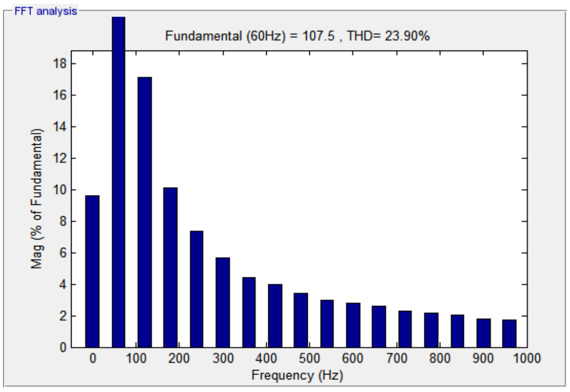

Fig. 14. THD of output voltage from the wind farm in the presence of STATCOM.

5. Conclusions

In this paper, the improvement of power profile and reactive power compensator using STATCOM in wind farms is analyzed. Without static compensation, the active power range is very small and the reactive power has large unchanged values that produce perturbations at the grid voltage. According to the simulation results, STATCOM is able to control the active power in a wide range and the reactive power output changes in the wind farm to an acceptable size. By using the appropriate output filter for STATCOM and selecting the optimal values for it, the quality of voltage and current waveforms is greatly improved. Furthermore, THD studies showed that using STATCOM, the amount of total harmonic distortion is greatly reduced and is within the IEEE standards for STATCOM.

References

[1] H. Tan, Z. Ren, W. Yan, Q. Wang and M. A. Mohamed, "A Wind Power Accommodation Capability Assessment Method for Multi-Energy Microgrids," in *IEEE Transactions on Sustainable Energy*, vol. 12, no. 4, pp. 2482-2492, Oct. 2021.

[2] M. N. Musarrat, A. Fekih and M. R. Islam, "An Improved Fault Ride Through Scheme and Control Strategy for DFIG-Based Wind Energy Systems," in *IEEE Transactions on Applied Superconductivity*, vol. 31, no. 8, pp. 1-6, Nov. 2021, Art no. 5401906.

[3] S. W. Ali et al., "Offshore Wind Farm-Grid Integration: A Review on Infrastructure, Challenges, and Grid Solutions," in *IEEE Access*, vol. 9, pp. 102811-102827, 2021.

[4] A. M. Ibrahim, S. A. Gawish, N. H. El-Amary and S. M. Sharaf, "STATCOM Controller Design and Experimental Investigation for Wind Generation System," in *IEEE Access*, vol. 7, pp. 150453-150461, 2019.

[5] Lin Wenjing, “The Algorithm Study of the

Controller in the Variable Speed Constant Frequency Doubly-Fed Wind Power Generation System," M.S. dissertation, Dept. Electronics and Electric Engineering., Univ. Shanghai Jiao Tong, 2008.

[6] H. Camblong, I. Martinez de Alegria, M. Rodriguez, and G. Abad, "Experimental evaluation of wind turbines maximum power point tracking controllers," *Energy Conversion and Management*, vol. 47, pp. 2846-2858, Nov. 2006.

[7] D. Santos-Martin, S. Arnaltes, and J.L. Rodriguez Amenedo, "Reactive power capability of doubly fed asynchronous generators," *Electric Power Systems Research*, vol. 78, pp. 1837-1840, Nov. 2008.

[8] Shen Hong, Wang Weisheng, and Dai Huizhu, "Reactive Power Limit of Variable-Speed Constant-Frequency Wind Turbine," *Power System Technology*, vol. 27, pp. 60-63, Nov. 2003.

[9] Yan Gangui, Wang Maochun, and Mugang, "Modeling of Grid-Connected Doubly-Fed Induction Generator for Reactive Power Static Regulation Capacity Study," *Transactions of China Electrotechnical Society*, vol. 23, pp. 98-104, Jul. 2008.

[10] Luis M. Fernández, Francisco Jurado, and José Ramón Saenz, "Aggregated dynamic model for wind farms with doubly fed induction generator wind turbines," *Renewable Energy*, vol. 33, pp. 129-140, Jan. 2008.

[11] Sergei P, Andrea T, and Alerto T, "Power control of a doubly fed induction machine via output feedback," *Control Engineering Practice*, vol. 12, pp. 41-57, Jan. 2004.

[12] Cai Zhi, Liu Jianzheng, and Wang Jian, "Simulation Research on Control Modes of Doubly-Fed Wind Power Generator Based on PSCAD," *Electrical Engineering*, pp. 61-64, 2008.

[13] P. Ju, B. Sun, M. Shahidehpour and X. Pan, "Impedance Modeling and Analysis for DFIG-Based Wind Farm in SSO Studies," in *IEEE Access*, vol. 8, pp. 158380-158390, 2020.

[14] Pooler M.A., "Doubly-fed induction machine models for stability assessment of wind farms," in *Proc. 2003 IEEE Int. Power Tech Conf.*, Italy.